*J Nutr Health Aging. 2019;23(8):739-745*



# DIET MODULATION RESTORES AUTOPHAGIC FLUX IN DAMAGED SKELETAL MUSCLE CELLS

F.M. GIORDANO[1], S. BURATTINI[1], F. BUONTEMPO[2], B. CANONICO[1], A.M. MARTELLI[2], S. PAPA[1], M. SAMPAOLESI[3,4], E. FALCIERI[1], S. SALUCCI[1]

1. Department of Biomolecular Sciences, University of Urbino Carlo Bo, Urbino, Italy; 2. Department of Biomedical and Neuromotor Sciences, University of Bologna, Bologna, Italy; 3. Translational Cardiomyology Laboratory, Stem Cell Institute of Leuven, Unit of Stem Cell Research, Cluster of Stem Cell and Developmental Biology, Department of Development and Regeneration, University of Leuven, Leuven, Belgium; 4. Human Anatomy Unit, Department of Public Health, Experimental and Forensic Medicine, University of Pavia, Pavia, Italy.
Corresponding author: Sara Salucci, Department of Biomolecular Sciences, University of Urbino Carlo Bo, Urbino, Italy, Email: sara.salucci@uniurb.it

**Abstract:** *Objectives:* Autophagy is a physiological and highly regulated mechanism, crucial for cell homeostasis maintenance. Its impairment seems to be involved in the onset of several diseases, including muscular dystrophies, myopathies and sarcopenia. According to few papers, chemotherapeutic drug treatment is able to trigger side effects on skeletal muscle tissue and, among these, a defective autophagic activation, which leads to the persistence of abnormal organelles within cells and, finally, to myofiber degeneration. The aim of this work is to find a strategy, based on diet modulation, to prevent etoposide-induced damage, in a model of in vitro skeletal muscle cells. *Methods*: Glutamine supplementation and nutrient deprivation have been chosen as pre-treatments to counteract etoposide effect, a chemotherapeutic drug known to induce oxidative stress and cell death. Cell response has been evaluated by means of morpho-functional, cytofluorimetric and molecular analyses. *Results*: Etoposide treated cells, if compared to control, showed dysfunctional mitochondria presence, ER stress and lysosomal compartment damage, confirmed by molecular investigations. *Conclusions*: Interestingly, both dietary approaches were able to rescue myofiber from etoposide-induced damage. Glutamine supplementation, in particular, seemed to be a good strategy to preserve cell ultrastructure and functionality, by preventing the autophagic impairment and partially restoring the normal lysosomal activity, thus maintaining skeletal muscle homeostasis.

**Key words:** Skeletal muscle cells, chemotherapy treatment, mitochondria dysfunctionality, ER stress, lysosomal activity.

## Introduction

In skeletal muscle, cell homeostasis is ensured by two different pathways, which can be considered as "survival mechanisms": the ubiquitin-proteasome system and the autophagy-lysosome system. These two proteolytic pathways are highly regulated and involved in muscle atrophy occurrence (1).

In particular, the autophagy-lysosome signaling seems to be crucial for removing dysfunctional organelles and unfolded proteins, thus preventing their accumulation within the cell. On the other hand, the ubiquitin-proteasome system is responsible for protein quality control (2) both under normal and pathological conditions (3). In recent years, researchers focused their attention on the relationship between autophagy and disease. Indeed, an autophagic flux impairment seems to be involved in the onset of several pathologies (4, 5) such as muscular dystrophies and myopathies (6, 7), cancer (8, 9), diabetes (10), Parkinson's, Alzheimer's, Huntington's disease (11) and LSDs – lysosomal storage disorder's (12). According to few papers in the literature, chemotherapeutic treatments are able to trigger skeletal muscle damage (13, 14).

Moreover, we and others have previously demonstrated that C2C12 myotubes treated with etoposide (Eto), a chemotherapeutic drug known to induce cell death and oxidative stress increase, undergo nuclear disruption, cytoplasmic shrinkage, organelle alterations (15-17) as well as functional muscle impairment (18, 19).

Therefore, to find new therapeutic strategies to counteract muscle damage induced by chemotherapeutic drug exposure, based on diet modulation, could represent an interesting investigation field for many researchers to prevent muscle wasting observed in cancer-treated patients.

Glutamine, a non-essential branched-chain amino acid, seems to exert a protective role in skeletal muscle cells exposed to stress-inducing triggers (20-22). On the other hand, nutrient deprivation could represent a possible way to reactivate a protective role of autophagy, as already described by De Palma et al., 2014 (23) in a murine muscular dystrophic model.

Here, an in vitro skeletal muscle cell line has been exposed to Eto, to mimic chemotherapeutic induced damage. To counteract Eto effects, glutamine supplementation (iperglut) and nutrient deprivation have been evaluated as protective pre-treatments before drug exposure. Morpho-functional, cytofluorimetric and molecular analyses have been carried out to confirm Eto toxicity and to verify if diet modulation could prevent Eto-induced damage in differentiated C2C12 cells.

*Received February 2, 2019*
*Accepted for publication April 15, 2019*
Published online August 30, 2019, http://dx.doi.org/10.1007/s12603-019-1245-3

## Materials and Methods

### *Cell Culture and treatments*

C2C12 differentiated cells were grown in flasks or on coverslips in dishes as previously described (15). Upon reaching approximately 80% of confluence, myotube formation was induced with differentiation medium (DM) as described by (24).

Cells were maintained at 37°C in humidified atmosphere with 5% $CO_2$, daily monitored with a Nikon Eclipse TE 2000-S inverted Microscope (IM) and photographed with a digital DN 100 Nikon system (25). Cells were processed for electron, confocal microscopy as well as for flow cytometric and molecular analyses at the end of the 7th day of differentiation (26).

### *Cell treatments*

Cell damage was induced by exposing myotubes to 50 $\mu$M Eto for 24h at the end of the 6th day of differentiation. Drug concentration was chosen on the basis of previous findings by our group (15, 17, 27).

Moreover, to counteract Eto induced damage, iperglut and 4h starvation were the chosen treatments.

In particular, iperglut condition was carried out doubling the glutamine percentage in the medium (2% instead of the standard 1%) and administrated it to cell culture starting from 0 day until 7 days of differentiation.

4h starvation was performed with the glutamine-free medium and serum. Cells at 6 days of differentiation were incubated with serum and glutamine free medium for 4h and then refreshed with complete medium until 7 days of differentiation.

### *Transmission Electron Microscopy (TEM)*

Both pellets and monolayers were analysed by means of TEM.

Samples were grown in flasks to get pellets and on coverslips in dishes to obtain monolayers. In both cases, specimens were rinsed with PBS and immediately fixed in situ with 2.5% glutaraldyde in 0.1M phosphate buffer for 45 minutes. Cells were gently scraped after 15 minutes and then centrifuged at 1200 rpm for 30 minutes (28). Post-fixation in 1% $OsO_4$ for 1h, alcohol dehydration and araldite inclusion were performed, as previously described (27). Monolayer embedding was carried out by inverting capsules full of resin on samples; coverslips were then removed in liquid nitrogen (17).

After uranyl acetate and lead citrate staining, thin sections (~ 0.5 $\mu$m) were observed by means of electron microscope.

### *Immunofluorescence analysis (IF)*

Cells were grown in a 12-well plate, fixed with 4% paraformaldehyde (PFA) in PBS for 15 minutes in the dark, rinsed with PBS and stored at 4°C until immunostaining.

Samples were permeabilized with 0.2% Triton X-100 in PBS, containing 1% bovine serum albumin (BSA). Donkey serum (1:10 dilution in PBS) was applied as blocking solution and specimens were incubated with primary antibodies (reported hereafter) overnight in PBS+1% BSA (29). Alexa Fluor-conjugated secondary donkey antibodies were used 1:500 in PBS supplemented with 1% BSA and the nuclei were stained with Hoechst 33342 (Sigma-Aldrich, 1:3000 in PBS). Images were collected using an Eclipse Ti inverted microscope (Nikon).

Primary antibodies and their dilutions were as follows: 1:4 mouse anti-MyHC (Developmental Studies Hybridoma Bank, DSHB, clone MF20), 1:300 mouse anti-ki67 (Abcam), 1:50 rabbit anti-MyoD (Abcam).

### *Flow Cytometry (FC)*

The cardiolipin-sensitive probe (NAO; Sigma-Aldrich) is able to monitor changes in mitochondrial lipids (15, 30, 31) and used at low concentrations, in living cells. It is an efficient fluorescent indicator for the peroxidation of cardiolipin, an inner mitochondrial membrane lipid. Cells were incubated with 150nM NAO for 15 minutes at 37°C in the dark and then acquired by FC using the appropriate fluorescence channels. 10,000 events for each condition were analyzed (16).

The tetramethylrhodamine ethyl ester (TMRE) has been used to focus on mitochondria functional status thank to its ability to selectively enter into mitochondria according to the Nernst equation (32, 33). Cells have been loaded with 40 nM TMRE at 37°C for 15 minutes and the analysis has been carried out under non-quenching conditions. The specificity of this analysis has been determined using the uncoupling agent CCCP (Sigma-Aldrich) which caused mitochondrial membrane depolarization with a sudden decrease of TMRE fluorescence. Cells have been treated for 30 minutes with 10mM CCCP, stained with TMRE is described, and then acquired by flow cytometry. Fluorescence intensity as the initial signal after background subtraction.

The endoplasmic reticulum (ER) stress has been detected by means of ER-Tracker Green (Thermo Fisher Scientific, Waltham, MA, USA). This is a live-cell stain highly selective for the ER. This stain consists of the green fluorescent BODIPY® FL dye and glibenclamide that binds to the sulphonylurea receptors of ATP-sensitive K+ channels which are prominent on the ER and have a critical role in ER luminal homeostasis. Indeed, ER K+ channels are involved in functions such as protein folding, apoptosis, and calcium homeostasis (34, 35). Cells have been incubated with 100 nM ER-Tracker Green for 30 minutes at 37 °C and subjected to flow cytometric analyses.

The Acridine Orange (AO) is a pH-sensitive dye, used to detect acidic vesicular organelle formation (36-38). Cells were washed and resuspendend in 0.5 ml of medium and then stained with AO 75 ng/ml, 15 minutes at 37°C. Red lysosomal and green cytoplasmatic fluorescences of 10,000 cells per sample were acquired by FC using the FL3 and FL1 channels respectively.

All FC data have been collected from three separate experiments and presented as mean ± SD.

### *Confocal Laser Scanning Microscopy (CLSM)*

Cells were grown, treated and processed for observations on coverslips in a 6-well plate.

Premo™ Autophagy Sensor LC3-GFP (Thermo Fisher Scientific) allows to detect the LC3 protein localization; cells were transduced following the protocol provided by the datasheet (Exc/Em= 488/520).

500 ng/ml AO were added directly to culture medium for 15 minutes at 37°C (39).

Observations were performed with a Leica TCS-SP5 confocal microscope, connected to a DMI 6000 CS Inverted Microscope (Leica Microsystems CMS Gmbh); pictures were analyzed using the Leica Application Suite Advanced Fluorescence (LAS AF) software (26).

### *Western Blotting*

Protein assay was performed using the Bio-Rad protein assay according to the manufacturer's instructions. Cells were lysed at 107/ml in RIPA lysis buffer containing the Complete Protease Inhibitor Cocktail (Thermo Fisher Scientific Inc., Rockford, IL, USA). Lysates were then briefly sonicated to shear DNA and reduce viscosity and boiled for 5 minutes with reducing sample buffer. Gradient gels (4%-20% acrylamide) were used (Bio-Rad, Hercules, CA, USA). Analysis with an antibody to β-actin documented equal protein loading. All the primary and secondary antibodies were from Cell Signaling Technology (Danvers, MA, USA). Proteins were detected using the ECL Westar ηC 2.0 reagent (Cyanagen, Bologna, Italy). The ChemiDoc-It2 Imaging System and the VisionWorksLS Software (UVP, LLC, Upland, CA, USA) were used to achieve images (39).

## Results

Control myotubes were multinucleated and revealed the presence of several long shaped mitochondria, organized myofibers and, occasionally, autophagic vacuoles (Fig. 1A-D). The evaluation of Myosin Heavy-Chain (MyHC) by means of IF staining, evidenced preserved control fibers with a typical elongated shape (Fig.1D). Fusion index, calculated on the basis of the ratio between the number of nuclei within myotubes and the total number of nuclei in a field, was about 60% (Fig. 1K), in agreement with others (40).

Cells treated with iperglut (Fig. 1E, G) or starvation (Fig. 1H, I) showed a preserved architecture with numerous mitochondria. Autophagic vacuoles were also observable, especially after starvation treatment.

Iperglut- (Fig.1F) or starvation (Fig.1J) -treated myotubes showed a morphology similar to control with a fusion index about of ~66% and 54% respectively (Fig. 1K).

Eto-treated fibers evidenced a diffuse damage characterized by cytoplasmic vacuolization (Fig. 2A), mitochondria alterations (Fig. 2C) and ER stress; the presence of abnormal autophagic structures, even as big as myonuclei, is observable (Fig. 2A, 2E, 2F). These mega-vacuoles sometimes were empty (Fig. 2G), with an evident cytoplasmic shrinkage which leaded, as a consequence, to a reduced fiber size and to myofiber degeneration.

**Figure 1**

Control (A-D), iperglut (E-G) and starved myotubes (H-J) observed at TEM (A-C, E, G, H, I) and at IF (D, F and J)

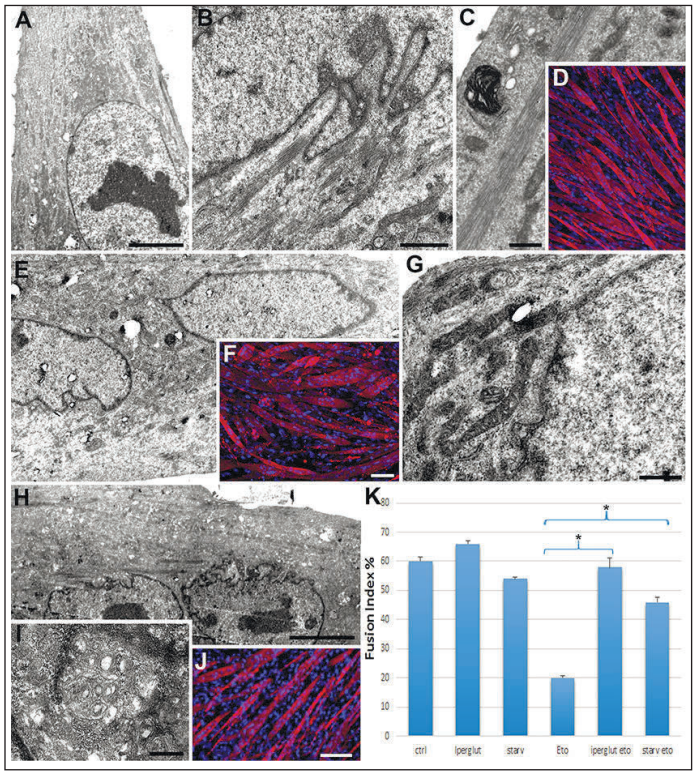


Micrographs show multinucleated cells with preserved mitochondria and cytoplasmic components. Sometimes autophagic vacuoles can be observed, particularly after starvation treatment. In K, the calculated fusion index of all experimental conditions is shown, expressed as mean±SD. For statistical analysis, Student t-test has been carried out. Both pre-treatments before drug vs Eto- treated myotubes are significant (* $p< 0.05$). Bars: 100 $\mu$m for D, F, J; 5 $\mu$m for A and H, 1 $\mu$m for B; 0.5 $\mu$m for C, G and I.

This behavior has been confirmed by IF staining. Eto-treated cells, indeed, displayed a strong reduction in terms of myotube number, which appeared small and thin (Fig.2B) with fusion index reduced to 20% or even less (Fig. 1K).

Iperglut pre-treatment, before Eto exposure, improved myotube morphology (Fig. 3A, C) if compared to Eto-treated cells; ER was similar to control and most of mitochondria appeared preserved. This morphology could be observed after IF too (Fig. 3B), where the calculated fusion index was about 58%, a percentage similar to control (Fig. 1K).

Starved cells, before Eto administration (Fig. 3D-F), retained their shape even if a diffuse cytoplasmic vacuolization, altered mitochondria and a conspicuous autophagic activation could

be observed. In this experimental condition, IF revealed an improvement of myotube morphology (Fig. 3G) and a calculated fusion index of about 46% (Fig. 1K).

**Figure 2**

Eto-treated myotubes observed by TEM (A, C-G) and IF (B)

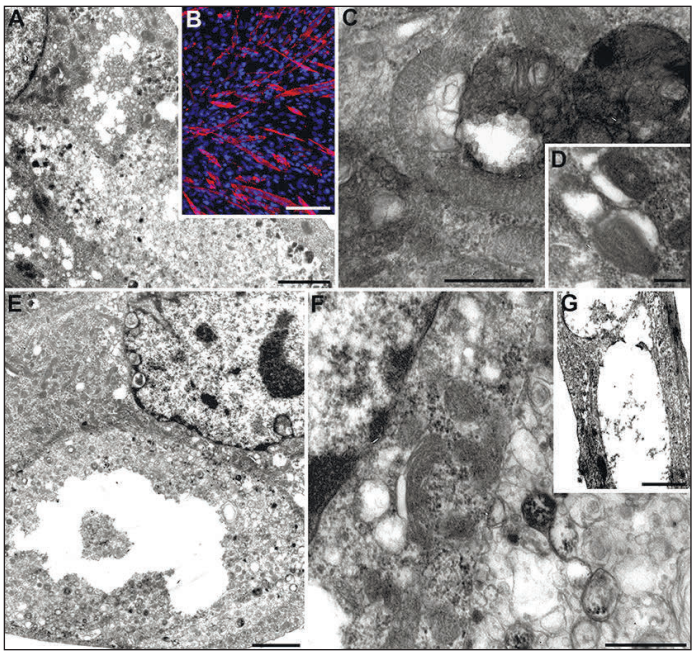


Cells display an evident damage of mitochondria and ER as well as the presence of abnormal vacuoles. IF analysis shows a reduced myotube size and number. Bars: 2 $\mu$m for A, E, G; 50 $\mu$m for B; 200 nm for C; 500 nm for C, F.

According to ultrastructural observations, FC analyses showed functional mitochondria in control condition and after iperglut supplementation. The presence of damaged-mitochondria could be observed after Eto administration, a chemotherapeutic agent able to activate also an oxidative pathway, as already reported by Salucci et al., 2013, 2016, 2017 (15-17). In this experimental condition, a high number of peroxidation events has been quantified by means of NAO staining (Fig 3H) and the analysis of TMRE/MTG ratio showed the presence of inactive and disrupted mitochondria (Fig. 3I). Iperglut or starvation administration before drug treatment reduced the presence of peroxidated cardiolipin and decreased TMRE/MTG ratio, suggesting that both pre-treatments were able to preserve mitochondrial viability.

Moreover, ER, the major site for the synthesis, folding and trafficking of secretory and membrane proteins, is known to be highly sensitive to redox status (41).

Here, ER state has been evaluated through FC, showing a MFI fluorescence increase (Fig. 3J) in case of starved and Eto-treated cells, if compared with other conditions. Dilated ER, absent in control condition (Fig. 3K), has been also observed after Eto exposure at TEM (Fig. 3L). Both pre-treatments, in particular iperglut, restored ER functionality (Fig. 3J) and morphology (Fig. 3M).

It is known that ER stress leads to activation of unfolded protein response (UPR) that acts as adaptive mechanisms to re-establish protein homeostasis (42). However, when the accumulation of unfolded/misfolded proteins occurs, Grp78/BiP, a major ER chaperone protein, critical for ER protein quality control, preferentially binds these proteins. As a consequence, ER stress response activation, including an up-regulation of genes encoding Grp78/BiP and a down-regulation of protein synthesis, occurs (43, 44). In this study, WB analysis (Fig. 3N) revealed that after starvation and Eto treatment, Grp78/BiP expression markedly increased compared with the other experimental conditions, for activating UPR, probably as an attempt to facilitate proper folding of misfolded proteins or to contribute to cell death.

**Figure 3**

Iperglut (A-C) and starved-myotubes (D-G) after TEM (A, C-F) and IF (B, G) observations. Both pre-treatments improve myotube morphology, which appears similar to control condition. Mitochondria (H, I) and ER (J) analyses, quantified by FC, reveal the presence of damaged mitochondria and altered ER after Eto exposure. Both pre-treatments before drug, in particular iperglut, rescues mitochondria and ER functionality. This latter finding has been also confirmed by TEM analysis which show preserved ER morphology in control (K) and in iperglut before Eto-treated cells (M). On the contrary, a dilated ER appears after Eto (L). WB analysis of BIP/Grp78 (N)

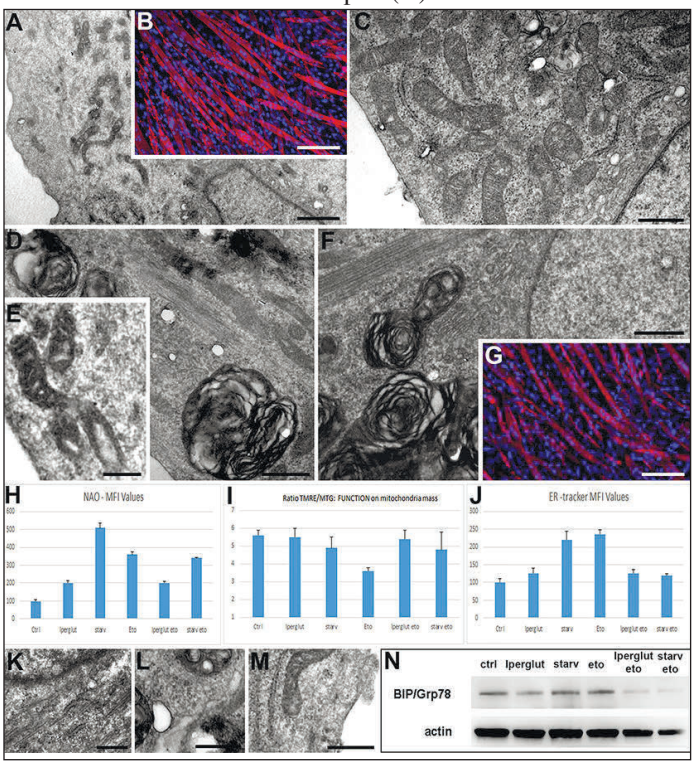


Bars: 1 $\mu$m for A; 0.5 $\mu$m for C, D, F, K, L, M; 200nm for E; 100 $\mu$m for B and G

**Figure 4**

Control and treated-samples after LC3 (A-F) and AO (G-M) staining observed by CLSM. LC3 dots are few in control cells (A), localize as little puncta near plasma membrane after iperglut treatment (B) and their number increases in starved myotubes (C). After Eto exposure, LC3 staining appears as large dots diffuse in the cytoplasm and often observed between myonuclei (D). Iperglut or starvation administration before Eto reduces the size of LC3 puncta (E, F) which appear again localized along plasma membrane. Preserved lysosomes (red fluorescence) appears in control (G), iperglut (H) and starved myotubes (I), stained with AO. Eto (J) induces an evident instability of lysosomal compartment (green fluorescence) which improves after iperglut (K, L) or starvation (M) pre-treatments before drug. AO quantification (N), through FC, confirms this behavior. In O, WB analysis of LC3, Beclin and p62 can be observed. Bars: 25 $\mu$m for A, G-M; 10 $\mu$m for B-F

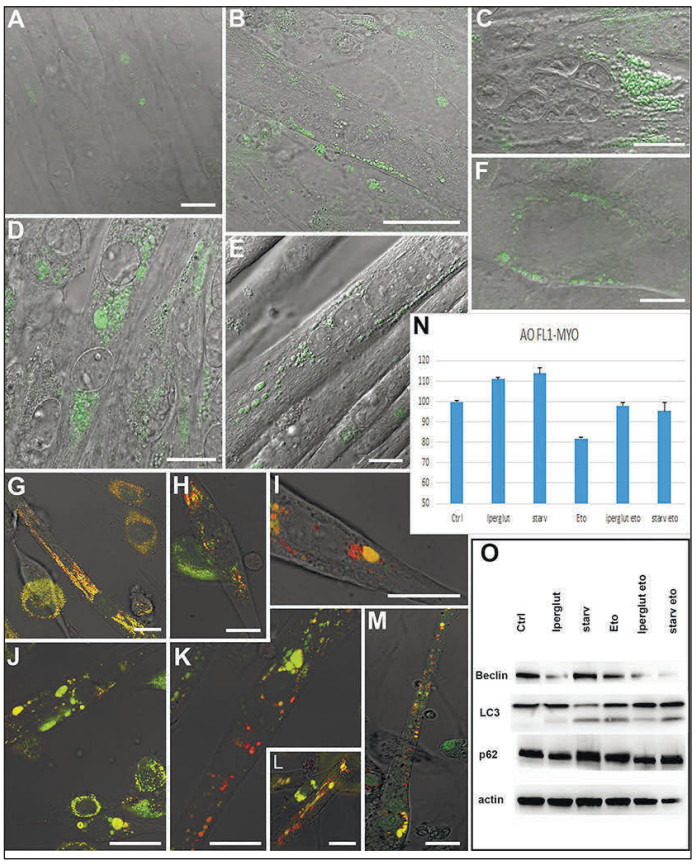


On the contrary, pre-treatments before chemotherapeutic drug exposure, maintained ER viability, as demonstrated by FC (Fig. 3J), TEM (Fig. 3M) and WB (Fig 3N) investigations.

Given the presence of a widespread autophagy, all samples have been stained with GFP-LC3 vector showing a slight presence of green spots in control condition (Fig 4A). Iperglut-differentiated myotubes (Fig. 4B) displayed a peripheral localization of small LC3 dots. On the contrary, starved cells (Fig. 4C) showed a diffuse cytoplasmic localization of LC3 protein.

Accumulation of LC3 protein as large green spots (Fig.4D) appeared in Eto-treated cells, confirming TEM observations.

Both pre-treatments (Fig. 4E, F) seemed to have beneficial effects on Eto-treated myotubes: LC3 puncta appeared small and localized as described in the control, without the large accumulation noticed after drug exposure.

AO staining, evaluated by CLSM (Fig. 4G-M) and quantified at FC (Fig. 4N), showed a good morphology and preservation of autophagy-lysosome system in control (Fig. 4G), iperglut (Fig. 4H) and starved myotubes (Fig. 4I). It appeared down-regulated after Eto exposure (Fig. 4J), suggesting a diffuse damage of autophagolysosomes and lysosomes. Iperglut (Fig. 4K, L) and starvation (Fig. 4M) treatments restored lysosomal functionality.

These findings have been then confirmed by WB analyses (Fig. 4O).

Beclin-1, a protein involved in the first phases of autophagy, appeared increased in starvation- and etoposide-treated cells compared with other conditions, suggesting an autophagic activation (45). In contrast, Beclin-1 expression decreased with either pre-treatment before drug exposure.

To analyze autophagy, the expression of the microtubule-associated protein 1 light chain 3B (LC3B), in particular, of the lipidated isoform II (LC3B-II) has been investigated. WB showed that LC3B-I protein levels were not significantly modified in all experimental conditions, while LC3B-II protein levels appeared increased in starved myotubes and in Eto-treated samples. These findings suggested either autophagosome formation or reduced autophagosome turnover (46). On the other hand, in iperglut pre-treated cells before Eto exposure, an LC3B-II reduction could be observed.

Finally, p62/SQSTM1 expression, involved in selectively targeting protein aggregates to autophagosomes by simultaneously binding LC3B and ubiquitinated proteins, has been evaluated (47). p62, constantly removed by autophagy, is considered a good marker for autophagic vesicle turnover evaluation (48). p62 is degraded during autophagy and therefore its level should decrease when autophagy is induced.

High levels of p62 protein (fig. 4O) appeared in samples treated with starvation and Eto, suggesting autophagosome clearance impairment, probably due to exhaustion of the lysosomal degradative capacity. Iperglut administration before Eto induced p62 content reduction, indicating a reactivation of the autophagic flux, necessary to counteract Eto damage and, as a consequence, to maintain myotube homeostasis.

## Discussion

Autophagy protects cells from stress (49) and plays a crucial role in the regulation of homeostatic processes (50, 51) by favoring the turnover of cell components and the clearance of damaged organelles through the autophagic-lysosomal pathway (52). It is known that excessive activation of autophagy-

dependent degradation contributes to muscle atrophy and cachexia. On the other hand, inhibition of autophagic flux causes accumulation of protein aggregates and abnormal organelles, leading to myofiber degeneration (53, 54).

In this study, two different culture conditions (iperglut or starvation) have been investigated in terms of restoring affected myotubes exposed to Eto. This chemical, as revealed by ultrastructure and cytofluorimetric analyses, induces mitochondrial damage, ER alteration, cardiolipin oxidation and accumulation of abnormal vacuoles in differentiated skeletal muscle cells. It induces also an increase of BIP, a known marker of ER stress; this parameter probably reflects a higher level of ROS, also confirmed by the presence of a mitochondrial population characterized by oxidized cardiolipin and loss of their functionality (55).

Moreover, CLSM observations reveal in Eto-treated myotubes an increase of LC3 puncta, absent in control samples, as fluorescent abnormal dots and an alteration of acid organelles stained with AO, which reflect the lysosomal instability. WB analysis show that chemotherapeutic drug induces an increase of two known markers of autophagosome formation such as Beclin1 and LC3-II; in additon, p62 expression results up-regulated in Eto-treated samples in agreement with several studies that, in general, have documented a p62 increase under oxidative stress conditions, thus indicating its accumulation inhibits the correct autophagic flux (56, 57).

Pre-treating myotubes before chemical exposure with iperglut, and to a lower extent with starvation, improves cell morphology: restored mitochondria, ER, and preserved lysosomes can be detected. Moreover, WB analysis evidences in iperglut or starved myotubes before drug, if compared with Eto-treated cells, a down-regulation of Beclin1, LC3II and p62 expression. p62 levels reduction indicates an increased autophagic flux (58, 59), confirmed by AO staining, which leads to an improvement of lysosomal compartment efficiency.

The autophagy–lysosomal pathway is an important player implicated in the turnover of organelles and long-lived proteins, as well as in the clearance of damaged cell components and the degradation of cell material in order to allow energy supply and cell survival during starvation and stress (60). In skeletal muscle, autophagy is a highly regulated process that can be beneficial or deleterious, depending on its activation levels and on cellular environment. Therefore, we could interpret our findings assuming that in Eto-treated cells, as well as in starved myotubes, the increase of Beclin1 and the LC3II indicate induction of autophagy. On the other and, the increase of p62 suggests a defective autophagosome clearance and turnover. This interpretation is in agreement with Masiero et al. 2010 (61) who demonstrated that an impairment of autophagic flux as well as its inhibition leads to protein accumulation, contributing to muscle degeneration.

Our findings also show that a modulation of culture conditions before chemical treatment, in particular iperglut administration, could exert a protective role in rescuing muscle fiber from degeneration induced by a chemotherapeutic trigger.

In conclusion, L-glutamine supplementation could be considered as a potential inducer of autophagic reactivation by maintaining skeletal muscle homeostasis under oxidative stress conditions and in some severe muscle disorders, including aging, characterized by an accumulation of autophagosomes, due to lysosomal function defects.

*Acknowledgments:* This work has been possible thanks to the DISB 2017 Enhancement Project of Urbino University. We would like to thank the researchers of the Translational Cardiomyology Laboratory (KU Leuven) for suggestions and support in IF analyses.

*Conflict of interest:* No conflict of interest;

## References

1. Sandri M, Coletto L, Grumati P, Bonaldo P: Misregulation of autophagy and protein degradation systems in myopathies and muscular dystrophies. J. Cell Sci 2013, 126: 5325–33. https://doi.org/10.1242/jcs.114041.
2. Damrauer JS, Stadler ME, Acharyya S, Baldwin AS, Couch ME, Guttridge DC: Chemotherapy-induced muscle wasting: association with NF-κB and cancer cachexia. Eur J Transl Myol 2018, 28(2): 7590. https://doi.org/10.4081/ejtm.2018.7590.
3. Lee Y, Lee HY, Gustafsson AB: Regulation of autophagy by metabolic and stress signaling pathways in the heart. J Cardiovasc Pharmacol 2012, 60: 118–124. doi: 10.1097/FJC.0b013e318256cdd0.
4. Levine B, Kroemer G: Autophagy in the pathogenesis of disease. Cell 2008, 132(1): 27–42. https://doi.org/10.1016/j.cell.2007.12.018.
5. Mizushima N, Levine B, Cuervo AM, Klionsky DJ: Autophagy fights disease through cellular self-digestion. Nature 2008, 451(7182):1069–1075. doi: 10.1038/nature06639.
6. Park YE, Hayashi YK, Bonne G, Arimura T, Noguchi S, Nonaka I, Nishino I: Autophagic degradation of nuclear components in mammalian cells. Autophagy 2009, 5(6): 795–804. https://doi.org/10.4161/auto.8901
7. Saha S, Panigrahi DP, Patil S, Bhutia SK: Autophagy in health and disease: A comprehensive review. Biomed Pharmacother 2018, 104: 85-495. https://doi.org/10.1016/j.biopha.2018.05.007.
8. Lu SZ, Harrison-Findik DD: Autophagy and cancer. World J Biol Chem 2013, 4(3): 64–70. doi: 10.4331/wjbc.v4.i3.64.
9. Henson E, Chen Y, Gibson S: EGFR family members' regulation of autophagy is at a crossroads of cell survival and death in cancer. Cancers (Basel) 2017, 9(4): pii: E27. https://doi.org/10.3390/cancers9040027.
10. Kang YH, Cho MH, Kim JY, Kwon MS, Peak JJ, Kang SW, Yoon SY, Song Y: Impaired macrophage autophagy induces systemic insulin resistance in obesity. Oncotarget 2016, 7(24): 35577–35591. https://doi.org/10.18632/oncotarget.9590.
11. Cheung ZH, Ip NY: Autophagy deregulation in neurodegenerative diseases – recent advances and future perspectives. J Neurochem 2011, 118(3): 317–325. https://doi.org/10.1111/j.1471-4159.2011.07314.x.
12. Settembre C, Fraldi A, Jahreiss L, Spampanato C, Venturi C, Medina D, de Pablo R, Tacchetti C, Rubinsztein DC, Ballabio A: A block of autophagy in lysosomal storage disorders. Hum Mol Genet 2008, 17(1): 119–29. https://doi.org/10.1093/hmg/ddm289.
13. Fanzani A, Zanola A, Rovetta F, Rossi S, Aleo MF: Cisplatin triggers atrophy of skeletal C2C12 myotubes via impairment of Akt signalling pathway and subsequent increment activity of proteasome and autophagy systems. Toxicol Appl Pharmacol 2011, 250(3), 312–321. https://doi.org/10.1016/j.taap.2010.11.003.
14. Stacchiotti A, Favero G, Giugno L, Lavazza A, Reiter RJ, Rodella LF, Rezzani R: Mitochondrial and metabolic dysfunction in renal convoluted tubules of obese mice: protectiverole of melatonin. PLoS One 2014, 9(10):e111141. https://doi.org/10.1371/journal.pone.0111141.
15. Salucci S, Burattini S, Baldassarri V, Battistelli M, Canonico B, Valmori A, Papa S, Falcieri E: The peculiar apoptotic behavior of skeletal muscle cells. Histol Histopathol 2013, 28(8), 1073–1087. doi: 10.14670/HH-28.1073.
16. Salucci S, Baldassarri V, Canonico B, Burattini S, Battistelli M, Guescini M, Papa S, Stocchi V, Falcieri E: Melatonin behavior in restoring chemical damaged C2C12 myoblasts. Microsc Res Tech 2016: 79(6), 532–540. doi: 10.1002/jemt.22663.
17. Salucci S, Battistelli M, Baldassarri V, Burini D, Falcieri, E, Burattini S: Melatonin prevents mitochondrial dysfunctions and death in differentiated skeletal muscle cells. Microsc Res Tech 2017, 80(11): 1174–1181. doi: 10.1002/jemt.22663.
18. Conte E, Camerino GM, Mele A, De Bellis M, Pierno S, Rana F, Fonzino A, Caloiero R, Rizzi L, Bresciani E, Ben Haj Salah K, Fehrentz JA, Martinez J, Giustino A, Mariggiò MA, Coluccia M, Tricarico D, Lograno MD, De Luca A, Torsello A, Conte D, Liantonio A: Growth hormone secretagogues prevent dysregulation of skeletal muscle calcium homeostasis in a rat model of cisplatin-induced cachexia. J Cachexia Sarcopenia Muscle, 2017, 8(3): 386–404. https://doi.org/10.1002/jcsm.12185.
19. Douglas E, McMillan DC: Towards a simple objective framework for the investigation and treatment of cancer cachexia: the Glasgow Prognostic Score. Cancer Treat Rev 2014, 40(6): 685–91. https://doi.org/10.1016/j.ctrv.2013.11.007.
20. Gaurav K, Goel RK, Shukla M, Pandey M: Glutamine: a novel approach to

chemotherapy-induced toxicity. Indian J Med Paediatr Oncol 2012, 33(1): 13–20. doi: 10.4103/0971-5851.96962.
21. Yoshida S, Kaibara A, Ishibashi N, Shirouzu K: Glutamine supplementation in cancer patients. Nutrition 2001, 17(9):766–768 https://doi.org/10.1016/S0899-9007(01)00629-3
22. Girven M, Dugdale HF, Owens DJ, Hughes DC, Stewart CE, Sharples AP:l-glutamine improves skeletal muscle cell differentiation and prevents myotube atrophy after cytokine (tnf-α) stress via reduced p38 mapk signal transduction. J Cell Physiol 2016, 231(12): 2720–2732. https://doi.org/10.1002/jcp.25380.
23. De Palma C, Perrotta C, Pellegrino P, Clementi E, Cervia D: Skeletal muscle homeostasis in duchenne muscular dystrophy: modulating autophagy as a promising therapeutic strategy. Front Aging Neurosci 2014, 6: 188. https://doi.org/10.3389/fnagi.2014.00188.
24. Battistelli M, Salucci S, Olivotto E, Facchini A, Minguzzi M, Guidotti S, Pagani S, Flamigni F, Borzì RM, Facchini A, Falcieri E: Cell death in human articular chondrocyte: a morpho-functional study in micromass model. Apoptosis 2014, 19(10): 1471–1483. doi: 10.1007/s10495-014-1017-9.
25. Burattini S, Salucci S, Baldassarri V, Accorsi A, Piatti E, Madrona A, Espartero JL, Candiracci M, Zappia G, Falcieri E: Anti-apoptotic activity of hydroxytyrosol and hydroxytyrosyl laurate. Food Chem Toxicol 2013, 55: 248–256. https://doi.org/10.1016/j.fct.2012.12.049.
26. Salucci S, Burattini S, Falcieri E, Gobbi P: Three-dimensional apoptotic nuclear behavior analyzed by means of Field Emission in Lens Scanning Electron Microscope. Eur J Histochem 2015, 59(3): 2539. doi: 10.4081/ejh.2015.2539.
27. Salucci S, Battistelli M, Burattini S, Squillace C, Canonico B, Gobbi P, Papa S, Falcieri E: C2C12 myoblast sensitivity to different apoptotic chemical triggers. Micron 2010, 41(8): 966–73. https://doi.org/10.1016/j.micron.2010.07.002
28. Burattini S, Battistelli M, Codenotti S, Falcieri E, Fanzani A, Salucci S: Melatonin action in tumor skeletal muscle cells: an ultrastructural study. Acta Histochem 2016, 118(3): 278-285. doi: 10.1016/j.acthis.2016.02.004.
29. Costamagna D, Quattrocelli M, van Tienen F, Umans L, de Coo IF, Zwijsen A, Huylebroeck D, Sampaolesi M: Smad1/5/8 are myogenic regulators of murine and human mesoangioblasts. J Mol Cell Biol 2016, 8(1): 73–87. https://doi.org/10.1093/jmcb/mjv059.
30. Luchetti F, Canonico B, Mannello F, Masoni C, D'Emilio A, Battistelli M, Papa S, Falcieri E: Melatonin reduces early changes in intramitochondrial cardiolipin during apoptosis in U937 cell line. Toxicol In Vitro 2007, 21: 293–301. https://doi.org/10.1016/j.tiv.2006.08.003
31. Canonico B, Campana R, Luchetti F, Arcangeletti M, Betti M, Cesarini, E, Ciacci C, Vittoria E, Galli L, Papa S, Baffone W: Campylobacter jejuni cell lysates differently target mitochondria and lysosomes on HeLa cells. Apoptosis 2014, 19: 1225–1242. https://doi.org/10.1007/s1049.
32. Ehrenberg B, Montana V, Wei MD, Wuskell JP, Loew LM: Membrane potential can be determined in individual cells from the nernstian distribution of cationic dyes. Biophys J 1998, 53: 785–794. https://doi.org/10.1016/S0006-3495(88)83158-8.
33. Luchetti F, Betti M, Canonico B, Arcangeletti M, Ferri P, Galli F, Papa S: ERK MAPK activation mediates the antiapoptotic signaling of melatonin in UVB-stressed U937 cells. Free Radic Biol Med 2009, 46: 339–351. https://doi.org/10.1016/j.freeradbiomed.2008.09.017.
34. Hogg RC, Adams DJ: An atp-sensitive k (+) conductance in dissociated neurones from adult rat intracardiac ganglia. J. Physiol 2001, 534: 713–720. https://doi.org/10.1111/j.1469-7793.2001.00713.x
35. Ghasemi M, Khodaei N, Salari S, Eliassi A, Saghiri R: Gating behavior of endoplasmic reticulum potassium channels of rat hepatocytes in diabetes. Iran. Biomed. J 2014, 18: 165–172. doi: 10.6091/ibj.13082.2014.
36. Thibodeau MS, Giardina C, Knecht DA, Helble J, Hubbard AK: Silica-induced apoptosis in mouse alveolar macrophages is initiated by lysosomal enzyme activity. Toxicol Sci 2004, 80(1), 34–48. https://doi.org/10.1093/toxsci/kfh121
37. Chen Y, Azad MB, Gibson SB: Methods for detecting autophagy and determining autophagy-induced cell death. Can J Physiol Pharmacol 2010, 88: 285–295. https://doi.org/10.1139/Y10-010.
38. Canonico B, Cesarini E, Salucci S, Luchetti F, Falcieri E, Di Sario G, Palma F, Papa S: Defective Autophagy, Mitochondrial Clearance and Lipophagy in Niemann-Pick Type B Lymphocytes. PLoS One 2016, 11(10): e0165780. https://doi.org/10.1371/journal.pone.0165780
39. Salucci S, Burattini S, Buontempo F, Martelli AM, Falcieri E, Battistelli M: Protective effect of different antioxidant agents in UVB-irradiated keratinocytes. Eur J Histochem 2017, 61(3), 2784. doi: 10.4081/ejh.2017.2784.
40. Gabillard JC, Sabin N, Paboeuf G: In vitro characterization of proliferation and differentiation of trout satellite cells. Cell Tissue Res. 2010, 342(3):471-7. doi: 10.1007/s00441-010-1071-8. Epub 2010 Nov 18.
41. Kwak HJ, Choi HE, Cheon HG: 5-LO inhibition ameliorates palmitic acid-induced ER stress, oxidative stress and insulinresistance via AMPK activation in murinemyotubes. Sci Rep 2017, 7(1): 5025. doi: 10.1038/s41598-017-05346-5.
42. Lee J, Ozcan U: Unfolded protein response signaling and metabolic diseases. J Biol Chem 2014, 289(3): 1203–1211. doi: 10.1074/jbcR113.534743.
43. Foti DM, Welihinda A, Kaufman RJ, Lee AS: Conservation and divergence of the yeast and mammalian unfolded protein response. Activation of specific mammalian endoplasmic reticulum stress element of the grp78/BiP promoter by yeast Hac1. J Biol Chem 1999, 274(43): 30402–30409. doi: 10.1074/jbc.274.43.30402
44. Bertolotti A, Zhang Y, Hendershot LM, Harding HP, Ron D: Dynamic interaction of BiP and ER stress transducers in the unfolded-protein response. Nat Cell Biol 2000, 2(6): 326–332. doi: 10.1038/35014014.
45. Aversa Z, Pin F, Lucia S, Penna F, Verzaro R, Fazi M, Colasante G, Tirone A, Rossi Fanelli, F, Ramaccini C, Costelli P, Muscaritoli M: Autophagy is induced in the skeletal muscle of cachectic cancer patients. Sci Rep 2016, 6: 30340. doi: 10.1038/srep30340.
46. Tanida I, Ueno T, Kominami E: LC3 conjugation system in mammalian autophagy. Int J Biochem Cell Biol 2004, 36(12) :2503–18. https://doi.org/10.1016/j.biocel.2004.05.009.
47. Kirkin V, McEwan DG, Novak I, Dikic I: A role for ubiquitin in selective autophagy. Mol Cell 2009, 34(3): 259–69. https://doi.org/10.1016/j.molcel.2009.04.026.
48. Klionsky DJ et al: Guidelines for the use and interpretation of assays for monitoring autophagy (3rd edition). Autophagy 2016, 12(1):1–222. doi: 10.1080/15548627.2015.1100356.
49. Saitoh T, Akira S: Regulation of innate immune responses by autophagy-related proteins. J Cell Biol 2010, 189(6):925–935. http://doi.org/10.1083/jcb.201002021.
50. Lee JA, Gao FB: ESCRT, autophagy, and frontotemporal dementia. BMB Rep 2008, 41(12): 827–832. doi: 10.1016/j.freeradbiomed.2017.07.017.
51. Levine B, Mizushima N, Virgin HW: Autophagy in immunity and inflammation. Nature 2011, 469(7330): 323–335. doi: 10.1038/nature09782.
52. Grumati P, Coletto L, Sabatelli P, Cescon M, Angelin A, Bertaggia E, Blaauw B, Urciuolo A, Tiepolo T, Merlini L, Maraldi NM, Bernardi P, Sandri M, Bonaldo P: Autophagy is defective in collagen VI muscular dystrophies, and its reactivation rescues myofiber degeneration. Nat Med 2010, 16(11), 1313–20. doi: 10.1038/nm.2247.
53. Romanello V, Sandri M: Mitochondrial Quality Control and Muscle Mass Maintenance. Front Physiol 2016, 6:422. doi: 10.3389/fphys.2015.00422.
54. Pollock N, Staunton CA, Vasilaki A, McArdle A, Jackson MJ: Denervated muscle fibers induce mitochondrial peroxide generation in neighboring innervatedfibers: Role in muscle aging. Free Radic Biol Med 2017, 112: 84–92. https://doi.org/10.1016/j.freeradbiomed.2017.07.017.
55. Pierre N, Barbé C, Gilson H, Deldicque L, Raymackers JM, Francaux M: Activation of ER stress by hydrogen peroxide in C2C12 myotubes. Biochem Biophys Res Commun. 2014, 450(1): 459–63. https://doi.org/10.1016/j.bbrc.2014.05.143.
56. Zheng YT, Shahnazari S, Brech A, Lamark T, Johansen T, Brumell JH: The adaptor protein p62/SQSTM1 targets invading bacteria to the autophagy pathway. J Immunol 2009, 183(9): 5909–16. https://doi.org/10.4049/jimmunol.0900441.
57. Park SY, Sun EG, Lee Y, Kim MS, Kim JH, Kim WJ, Jung JY: Autophagy induction plays a protective role against hypoxic stress in human dental pulp cells. J Cell Biochem 2018, 119(2): 1992–2002. https://doi.org/10.1002/jcb.26360.
58. Bjørkøy G, Lamark T, Pankiv S, Øvervatn A, Brech A, Johansen T: Monitoring autophagic degradation of p62/SQSTM1. Methods Enzymol 2009, 452: 181–97. https://doi.org/10.1016/S0076-6879(08)03612-4.
59. Lesmana R, Sinha RA, Singh BK, Zhou J, Ohba K, Wu Y, Yau WW, Bay BH, Yen PM: Thyroid Hormone Stimulation of Autophagy Is Essential for Mitochondrial Biogenesis and Activity in Skeletal Muscle. Endocrinology 2016, 157(1):23–38. https://doi.org/10.1210/en.2015-1632.
60. Glick D, Barth S, Macleod KF: Autophagy: cellular and molecular mechanisms. J Pathol 2010, 221(1), 3–12. https://doi.org/10.1002/path.2697.
61. Masiero E, Sandri M: Autophagy inhibition induces atrophy and myopathy in adult skeletal muscles. Autophagy 2010, 6(2): 307–309. doi: 10.4161/auto.6.2.11137.